

# Shearing approach to gauge invariant Trotterization

Jesse R. Stryker\*

Maryland Center for Fundamental Physics, University of Maryland, College Park, MD 20742, USA

(Dated: May 26, 2021)

Universal quantum simulations of gauge field theories are exposed to the risk of gauge symmetry violations when it is not known how to compile the desired operations exactly using the available gate set. In this letter, we show how time evolution can be compiled in an Abelian gauge theory—if only approximately—without compromising gauge invariance, by graphically motivating a block-diagonalization procedure. When gauge invariant interactions are associated with a “spatial network” in the space of discrete quantum numbers, it is seen that cyclically shearing the spatial network converts simultaneous updates to many quantum numbers into conditional updates of a single quantum number: ultimately, this eliminates any need to pass through (and acquire overlap onto) unphysical intermediate configurations. Shearing is explicitly applied to gauge-matter and magnetic interactions of lattice QED. The features that make shearing successful at preserving Abelian gauge symmetry may also be found in non-Abelian theories, bringing one closer to gauge invariant simulations of quantum chromodynamics.

The real-time dynamics of quantum field theories (QFTs) holds the details of rich nonperturbative physics, such as the fragmentation of jets at the Large Hadron Collider or early-universe bubble nucleation in extensions of the Standard Model. Analytic methods that can quantitatively predict nonperturbative phenomena from the underlying quantum field theories are scarce, and this deficit underlies the existence of what is today a sophisticated, numerical lattice QFT program. For decades, the lattice QFT program has pushed the envelope of high-performance computing and fundamental physics, but its scope has generally been restricted to properties for which a QFT’s Euclidean or imaginary-time path integral is not hampered by a sign problem. The calculation of real-time dynamics has largely been precluded by sign problems, except for special cases [1, 2]. The fact is that real-time dynamics explicitly involves events in Minkowskian, rather than Euclidean, spacetime. Any general computational solution—if one exists—will require the use of nontraditional lattice methods.

In recent years, a new computational avenue for dynamics has opened up [3–15] based on simulating field theoretic degrees of freedom [16–64] and their interactions with laboratory-controllable quantum systems, i.e., quantum simulators and computers [65, 66]. Quantum computers are naturally suited for simulating Hamiltonian mechanics, as opposed to path integrals, and thereby appear to be sign problem-free. This letter is specifically concerned with simulation by universal digital quantum computers (as opposed to analog ones, as well as quantum annealers), which are the model for architectures like those being engineered by Google [67], IBM [68], IonQ [69], Rigetti [70], and others.

Digital quantum simulation requires a quantum algorithm or set of instructions to be executed by the quantum computer. For QFTs, this may entail truncating and mapping the field degrees of freedom onto quantum bits (qubits) and mimicking Schrödinger-picture time evolu-

tion through an appropriate sequence of unitary gates. At the end of the evolution, measurements would be made to extract the observables of interest. How exactly QFTs and their dynamics would best be “digitized” is a subject of active research [7, 12, 15, 19, 21, 30, 35, 36, 43, 44, 60, 63, 71–74].

Among field theories that will be studied by quantum computers, gauge theories such as quantum chromodynamics are uniquely complex due to their hallmark local constraints — namely gauge invariance, which is identified with Gauss’s law and charge conservation. Unlike certain analog devices, in which there can be opportunities to map gauge symmetry to a physical symmetry of the simulator [58], qubits and the operations done on them generally do not discriminate between gauge-violating interactions and gauge-conserving ones. Gauge symmetry, therefore, is a concern for both the wave functions and the effectively simulated interactions. We do note, however, that there is evidence of dynamical robustness against gauge-violating interactions in certain contexts [75, 76]. Unless these observations can be extended to and made rigorous for more general gauge theories (particularly in the continuum limit), manifestly gauge invariant protocols, where possible and practical, remain preferable.

Symmetry preservation aside, a crucial consideration in selecting any QFT digitization is the implementation of its time evolution. Gauge theory Hamiltonians are often given in the form  $H = \sum_j H_j$ , where each  $H_j$  is a manifestly gauge invariant operator involving fields from a site, link, or unit square (plaquette) of a spatial lattice. The time evolution operator  $e^{-itH}$  generally will not be a native operation and must be constructed from the available gate set. The simplest and most well-studied approaches take advantage of Lie-Trotter-Suzuki product formulas [77–79]: at first order,  $e^{-itH} \simeq \left[ \prod_j e^{-itH_j/s} \right]^s$  for a sufficiently large number of Trotter steps,  $s$ . This *Trotterization* of the time evolution operator is inexact

for finite  $s$ , but it is gauge invariant because each  $H_j$  is.

In practice, the complexity of the  $H_j$  may call for a second level of approximation:  $e^{-i\delta t H_j} \rightarrow \prod_k V_{jk}(\delta t)$  in the limit of small  $\delta t$ , where each factor  $V_{jk}(\delta t)$  is an implementable sequence of elementary gates. There is no reason to expect *a priori* that the individual  $V_{jk}$  will be gauge invariant, nor is there any guarantee  $\prod_k V_{jk}(\delta t)$  conserves gauge symmetry either. Protecting gauge invariance through this second layer of approximation (which is also referred to as Trotterization) is a nontrivial aspect of designing the quantum circuit.

In this letter, a solution is introduced for Trotterizing Abelian gauge theories while preserving gauge symmetry. This is achieved by finding collections  $V_{jk}(\delta t)$  that *are* individually gauge invariant, implying gauge invariant time evolution. The key insight is that the transitions induced by gauge invariant operators can be thought of as a geometric graph or “spatial network” of parallel edges. Through appropriate changes of basis, the edges can be aligned parallel to the axis of a single quantum number, effectively turning the problem of tightly correlated transitions of multiple quantum numbers into transitions of a single quantum number conditioned by Boolean logic. This method, based on ‘cyclic shears,’ is illustrated by applying it to hopping terms (minimally-coupled fermion-photon interactions) and plaquette operators encountered in compact  $U(1)$  gauge theories, such as lattice QED.

*U(1) hopping terms.*—In Ref. [38], complete and scalable algorithms with bounded errors were given for time evolution of the lattice Schwinger model (QED in 1D space), truncated in the basis of electric fields and fermion occupation numbers. The  $H_j$  were link-localized electric energies and hopping terms, and site-localized mass terms. The propagators  $e^{-itH_j/s}$  associated to the electric and mass terms could be decomposed straightforwardly and exactly using typical universal gate sets because they are diagonal in the computational basis. The off-diagonal hopping terms do not enjoy the same benefit, making it less obvious how to exactly decompose their associated propagators as circuits.

Concretely, let  $\hat{\psi}$  and  $\hat{\chi}$  be the fermionic modes at two neighboring lattice sites,  $\hat{U}$  the gauge link variable joining them,  $x > 0$  the interaction strength, and  $\hat{T}_{\text{hop}} = x \hat{\psi}^\dagger \hat{\chi} \hat{U}$  the associated hopping term. Conjugate to a link operator is the integer electric field  $\hat{E}$  along that link; we work in the eigenbasis of  $\hat{E}$ , with  $\hat{U} = \sum_E |E+1\rangle \langle E|$ . We also assume a hard cutoff for which  $E_{\min} \leq E \leq E_{\max}$  and  $\hat{U} |E_{\max}\rangle = \hat{U}^\dagger |E_{\min}\rangle = 0$ .

A Jordan-Wigner transformation can be used to turn the fermionic operators into qubit (spin  $\frac{1}{2}$ ) operators, e.g.,

$$\hat{T}_{\text{hop}} = x \sigma_\psi^- \sigma_\chi^+ \hat{U}; \quad (1)$$

we are using a computational basis in which  $\sigma^+ = |0\rangle \langle 1|$  and 0 and 1 denote eigenvalues of  $\hat{n}_\psi \equiv \hat{\psi}^\dagger \hat{\psi}$  or  $\hat{n}_\chi \equiv \hat{\chi}^\dagger \hat{\chi}$ .

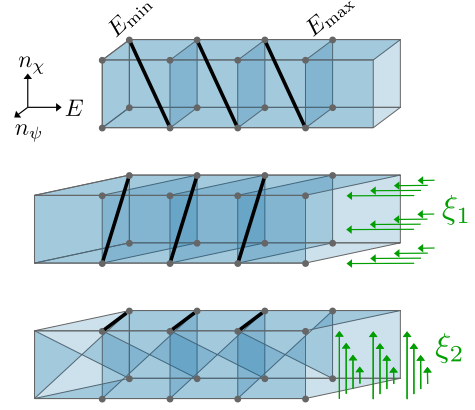


FIG. 1. Graphical representation of the transitions induced by hopping terms. Top: The transitions before any change of basis. Middle: The transitions after  $\hat{\xi}_1$ . Bottom: The transitions after  $\hat{\xi}_2 \hat{\xi}_1$ .

Electric eigenstates, truncated to  $\eta$  qubits per link, are interchangeably labelled by nonnegative integers  $\mathcal{E} = E - E_{\min}$ . Arithmetic involving  $\hat{\mathcal{E}}$  is always modulo  $2^\eta$ .

In multiqubit quantum computation, it is common for *Pauli operator* to refer to any tensor product of Pauli matrices  $I$ ,  $X$ ,  $Y$ , or  $Z$  acting on individual qubit spaces (e.g.,  $X \otimes X$  or  $I \otimes Z \otimes Z$ ). Pauli operators form a Hermitian basis for all multiqubit operators. The expression of an operator with respect to this basis is its *Pauli decomposition*. The exponential of a Pauli operator is considered easy to simulate, but directly Trotterizing the Pauli decomposition can be prohibitively inefficient. Generally, one will divide up and manipulate different parts of the Hamiltonian before arriving at Pauli operators intended for hardware implementation.

Diagonalized operators such as  $\hat{E}^2$  in the Schwinger model are trivial to program without approximation because Trotterizing their Pauli decomposition incurs no commutation errors:  $[I, Z] = 0$ . The off-diagonal hopping terms, however, are not as trivial to implement exactly, in part due to  $[X, Y] \neq 0$ . Diagonalizing the involved field operators is not an option since they are nilpotent. The fields’ Hermitian and antihermitian parts are of course diagonalizable, but they are not by themselves gauge covariant and they fail to commute. Ref. [38] went forward with the Hermitian and antihermitian fields, postponing the construction of fully gauge invariant Trotter steps.

Insight into the computational nature of gauge invariant transitions can be gained by graphically examining the structure of hopping terms as a whole within the space of quantum numbers. The top panel of Fig. 1 depicts the transitions induced by  $\hat{T}_{\text{hop}}$  and  $\hat{T}_{\text{hop}}^\dagger$  as edges in the  $(n_\psi, n_\chi, E)$  space of quantum numbers (shown for  $\eta = 2$ ). An edge connecting  $(n_\psi^i, n_\chi^i, E^i)$  and  $(n_\psi^f, n_\chi^f, E^f)$  corresponds to a nonzero matrix ele-

ment  $\langle n_\psi^f, n_\chi^f, E^f | (\hat{T}_{\text{hop}} + \hat{T}_{\text{hop}}^\dagger) | n_\psi^i, n_\chi^i, E^i \rangle$ . The transitions form what is known in graph theory as a geometric graph or spatial network. This particular spatial network consists of parallel edges whose slant represents simultaneous changes to all three relevant quantum numbers – as given, hopping terms are off-diagonal on all three field registers.

If the edges were instead oriented parallel to one of the axes, the interaction would be off-diagonal on a single register only. Such a block-diagonalization would make it easier to avoid most gauge-violating transitions by simply excluding all  $X$  and  $Y$  operations on the other registers' qubits. It is clear from Fig. 1 that this scenario is entirely attainable by appropriately shearing the graph.

The middle section of Fig. 1 show the result of a ‘cyclic shear’ transformation, which is mathematically given by

$$\hat{\xi}_1 = \delta_{\hat{n}_\psi, 0} + \delta_{\hat{n}_\psi, 1} \hat{\lambda}^- , \quad (2)$$

$$\hat{\xi}_1 \hat{T}_{\text{hop}} \hat{\xi}_1^\dagger = x \sigma_\psi^- \sigma_\chi^+ (1 - \delta_{\hat{E}, E_{\text{max}}}) . \quad (3)$$

Above,  $\delta_s$  serve as shorthand for projection operators:  $\delta_{\hat{n}_\psi, 0} = (|0\rangle\langle 0|)_\psi$ ,  $\delta_{\hat{E}, E_{\text{max}}} = |E_{\text{max}}\rangle\langle E_{\text{max}}|$ , etc. We also introduce cyclic incrementers  $\hat{\lambda}^\pm = \sum_{\mathcal{E}=0}^{2^\eta-1} |\mathcal{E} \pm 1\rangle\langle \mathcal{E}|$ . The ‘cyclicity’ of the shear transformation thus means that when a node gets sheared beyond the extent of its range, it wraps around to the opposite boundary and continues being sheared. In this way, the shears provide unitary mappings that can be applied to computational basis states.

Under  $\hat{\xi}_1$ ,  $\hat{T}_{\text{hop}}$  becomes off-diagonal on two registers only. This can then be combined with another shear,

$$\hat{\xi}_2 = \delta_{\hat{n}_\psi, 0} + \delta_{\hat{n}_\psi, 1} X_\chi , \quad (4)$$

$$\hat{\xi}_2 (\hat{\xi}_1 \hat{T}_{\text{hop}} \hat{\xi}_1^\dagger) \hat{\xi}_2^\dagger = x \delta_{\hat{n}_\chi, 1} \sigma_\psi^- (1 - \delta_{\hat{E}, E_{\text{max}}}) .$$

After the combined transformation  $\hat{\xi}_2 \hat{\xi}_1$ ,  $\hat{T}_{\text{hop}}$  becomes off-diagonal on the space of a single qubit. The projector  $(1 - \delta_{\hat{E}, E_{\text{max}}})$  that has arisen is necessary to prevent a reduced set of possible gauge-violating errors: those that correspond to wrap-around effects at the cutoffs. This is the work left to be done by hand, as far as charge conservation is concerned.

Fortuitously, in this case of gauge-fermion hopping terms, the work left to be done by hand is negligible. The Hermitian operator to be simulated,  $\delta_{\hat{n}_\chi, 1} X_\psi (1 - \delta_{\hat{E}, E_{\text{max}}})$ , can be implemented with two controlled  $X$ -rotations. Figure 2 shows these gates sandwiched between the shears. This circuit, which was only tailor-made to conserve charge, is actually an exact gate decomposition for the hopping propagator.

*Compact  $U(1)$  plaquettes.*—The shearing of plaquettes is explained below by first considering a toy model, two-link ‘plaquette’: two links joined end to end. The toy plaquette highlights every key feature of solving plaquette operators using shears, but is more easily visualized

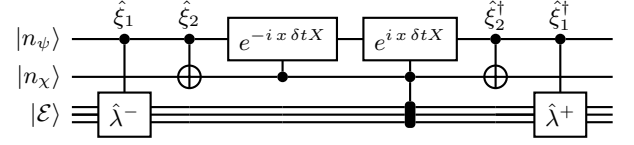


FIG. 2. Circuit to simulate a gauge-fermion hopping term  $x(\psi^\dagger \hat{\chi} \hat{U} - \psi \hat{\chi}^\dagger \hat{U}^\dagger)$ . The multiqubit electric register could be any number of qubits.

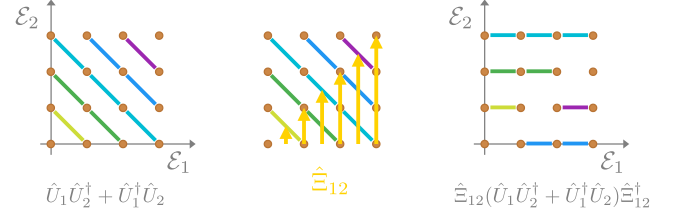


FIG. 3. Left: Applications of  $\hat{U}_1 \hat{U}_2^\dagger$  and  $\hat{U}_1^\dagger \hat{U}_2$  can only move a state by  $\pm(1, -1)$  in the 12-plane, forming chains of reachable states. The available chains are each displayed in a distinct color (shown here for  $\eta = 2$ ). Right: In the cyclically sheared electric coordinates, allowed moves generated by  $\hat{U}_1 \hat{U}_2^\dagger$  and  $\hat{U}_1^\dagger \hat{U}_2$  are parallel to the  $\mathcal{E}_1$ -axis.

than the case of four links. The generalization to the four-link plaquette is summarized thereafter.

Consider two links labeled ‘1’ and ‘2’ with their truncated ‘plaquette’ operator given by

$$\begin{aligned} \hat{U}_1 \hat{U}_2^\dagger &= \hat{\lambda}_1^+ [1 - \delta_{\hat{E}_1, E_{\text{max}}}] \hat{\lambda}_2^- [1 - \delta_{\hat{E}_2, E_{\text{min}}}] \\ &= \hat{\lambda}_1^+ \hat{\lambda}_2^- [1 - \delta_{\hat{\mathcal{E}}_1, -1}] [1 - \delta_{\hat{\mathcal{E}}_2, 0}] . \end{aligned} \quad (5)$$

A consequence of  $[\hat{U}_1 \hat{U}_2^\dagger, \hat{E}_1 + \hat{E}_2] = 0$  is that the electric configurations that can be mixed by  $\hat{U}_1 \hat{U}_2^\dagger$  lie on various one-dimensional lines in the space of electric quantum numbers. As illustrated in Fig. 3, these transitions can be aligned with one axis by a shear in the 12-plane:

$$\hat{\Xi}_{12} \equiv \sum_{j=0}^{2^\eta-1} \delta_{\hat{\mathcal{E}}_1, j} (\hat{\lambda}_2^+)^j . \quad (6)$$

Computationally,  $\hat{\Xi}_{12}$  is nothing but addition modulo  $2^\eta$ :  $|\mathcal{E}_1\rangle |\mathcal{E}_2\rangle \xrightarrow{\hat{\Xi}_{12}} |\mathcal{E}_1\rangle |\mathcal{E}_2 + \mathcal{E}_1\rangle$ . Applying  $\hat{\Xi}_{12}$  to the operators appearing in (5), we find that  $\hat{\lambda}_2^-$  and  $\hat{\mathcal{E}}_1$  are invariant, whereas  $\hat{\lambda}_1^+ \xrightarrow{\hat{\Xi}_{12}} \hat{\lambda}_1^+ \hat{\lambda}_2^+$  and  $\hat{\mathcal{E}}_2 \xrightarrow{\hat{\Xi}_{12}} \hat{\mathcal{E}}_2 - \hat{\mathcal{E}}_1$ . Therefore

$$\hat{\Xi}_{12} \hat{U}_1 \hat{U}_2^\dagger \hat{\Xi}_{12}^\dagger = \hat{U}_1 [1 - \delta_{\hat{\mathcal{E}}_2 - \hat{\mathcal{E}}_1, 0}] , \quad (7)$$

which is off-diagonal on register 1 alone.

To simulate the right-hand side of (7), we can up-cycle a strategy used in [38]. The identity  $\hat{\lambda}^\pm = \sigma_\mp^{(\text{lsb})} + \hat{\lambda}^+ \sigma_\mp^{(\text{lsb})} \hat{\lambda}^-$ , where  $\sigma_{\text{lsb}}^\pm$  acts on the least signif-

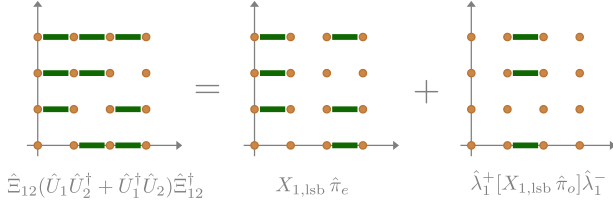


FIG. 4. The edges representing  $\hat{U}_1\hat{U}_2^\dagger + \text{H.c.}$  can be grouped by the even-odd parity of the column they are in, corresponding to the terms  $\hat{h}_e$  and  $\hat{h}_o$ .

icant (qu)bit of  $\mathcal{E}$ , is used in (7) to obtain

$$\hat{U}_1\hat{U}_2^\dagger + \hat{U}_1^\dagger\hat{U}_2 \xrightarrow{\Xi_{12}} \hat{h}_e + \hat{h}_o, \quad (8)$$

$$\begin{aligned} \hat{h}_e &= \hat{\pi}_e X_1^{(\text{lsb})}, \\ \hat{\pi}_e &\equiv (1 - \delta_{\hat{\mathcal{E}}_2, 2\lfloor \hat{\mathcal{E}}_1/2 \rfloor}), \\ \hat{h}_o &= \hat{\lambda}_1^+ \hat{\pi}_o X_1^{(\text{lsb})} \hat{\lambda}_1^-, \\ \hat{\pi}_o &\equiv (1 - \delta_{2\lfloor \hat{\mathcal{E}}_1/2 \rfloor + 1, -1})(1 - \delta_{\hat{\mathcal{E}}_2, 2\lfloor \hat{\mathcal{E}}_1/2 \rfloor + 1}). \end{aligned} \quad (9)$$

The projection operator  $\hat{\pi}_e$  ( $\hat{\pi}_o$ ) is named as such because it explicitly depends on  $\mathcal{E}_1$  rounded down (up) to the nearest even (odd) integer; in particular,  $\hat{\pi}_e$  and  $\hat{\pi}_o$  each commute with  $X_1^{(\text{lsb})}$ . Figure 4 provides intuition for the identity  $\hat{\Xi}_{12}(\hat{U}_1\hat{U}_2^\dagger + \hat{U}_1^\dagger\hat{U}_2)\hat{\Xi}_{12}^\dagger = \hat{h}_e + \hat{h}_o$  by interpreting the graph as a linear combination of pairwise mixings. The two terms correspond to a so-called ‘‘coloring’’ of the graph, for which the chromatic number is 2. The isolation of the terms  $\hat{h}_e$  and  $\hat{h}_o$  has the effect of breaking up chains of states connected by powers of the sheared plaquette into pairwise transitions in two-state subspaces; in  $\hat{h}_e$  they are bit-flips of the least significant bit, and the same can be said for  $\hat{h}_o$  if the basis is shifted by one unit. The projectors  $\hat{\pi}_e$  and  $\hat{\pi}_o$  that arise serve to prevent unphysical wrap-around effects at the cutoffs.

Next, we consider a first-order Trotterization  $e^{-i\delta t(\hat{U}_1\hat{U}_2^\dagger + \hat{U}_1^\dagger\hat{U}_2)} \simeq \hat{\Xi}_{12}^\dagger e^{-i\delta t\hat{h}_o} e^{-i\delta t\hat{h}_e} \hat{\Xi}_{12}$ , which incurs error due to  $[\hat{h}_e, \hat{h}_o] \neq 0$ , but respects gauge invariance. Now all that is needed is circuits for the Trotter factors

$$\exp[-i\delta t\hat{h}_o] = \hat{\lambda}_1^+ \exp[-i\delta t\hat{\pi}_o X_1^{(\text{lsb})}] \hat{\lambda}_1^-, \quad (10)$$

$$\exp[-i\delta t\hat{h}_e] = \exp[-i\delta t\hat{\pi}_e X_1^{(\text{lsb})}]. \quad (11)$$

At the heart of each factor is an  $X$ -rotation on register 1’s least significant bit, controlled by the other  $\eta - 1$  bits as dictated by  $\hat{\pi}_e$  or  $\hat{\pi}_o$ . Figure 5 shows a possible circuit implementation of the Trotterized hopping propagator for the case of  $\eta = 3$ . Protocols for  $\hat{\lambda}^\pm$  and  $\hat{\Xi}_{12}$  are left up to the user. The routine calls for two ancilla qubits.

Moving on, we now generalize to the case of four links ‘0,’ ‘1,’ ‘2,’ and ‘3.’ The truncated plaquette operator is

$$\hat{U}_\square = \hat{U}_0\hat{U}_1\hat{U}_2^\dagger\hat{U}_3^\dagger = \hat{\lambda}_0^+\hat{\lambda}_1^+\hat{\lambda}_2^-\hat{\lambda}_3^-[1 - \delta_{\hat{\mathcal{E}}_0, -1}][1 - \delta_{\hat{\mathcal{E}}_1, -1}]\times [1 - \delta_{\hat{\mathcal{E}}_2, 0}][1 - \delta_{\hat{\mathcal{E}}_3, 0}]. \quad (12)$$

Like before, the gauge invariant moves by  $\pm(1, 1, -1, -1)$  in the  $(E_0, E_1, E_2, E_3)$  hypercube induced by plaquettes form parallel chains in the space of quantum numbers that can be cyclically sheared to align with a single axis.

First, the  $E_0$  and  $E_3$  components of the moves can be eliminated by shears in the 01- and 23-planes:

$$\hat{\Xi}_{01} \equiv \sum_{j=0}^{2^n-1} \delta_{\hat{\mathcal{E}}_1, j} (\hat{\lambda}_0^-)^j, \quad (13)$$

$$\hat{\Xi}_{01}\hat{U}_0\hat{U}_1\hat{\Xi}_{01}^\dagger = \hat{U}_1(1 - \delta_{\hat{\mathcal{E}}_0 + \hat{\mathcal{E}}_1, -1}),$$

$$\hat{\Xi}_{23} \equiv \sum_{k=0}^{2^n-1} \delta_{\hat{\mathcal{E}}_2, k} (\hat{\lambda}_3^-)^k, \quad (14)$$

$$\hat{\Xi}_{23}\hat{U}_2^\dagger\hat{U}_3^\dagger\hat{\Xi}_{23}^\dagger = \hat{U}_2^\dagger(1 - \delta_{\hat{\mathcal{E}}_3 + \hat{\mathcal{E}}_2, 0}).$$

Combining the two,  $\hat{U}_\square$  is transformed into  $\hat{U}_1\hat{U}_2^\dagger(1 - \delta_{\hat{\mathcal{E}}_0 + \hat{\mathcal{E}}_1, -1})(1 - \delta_{\hat{\mathcal{E}}_3 + \hat{\mathcal{E}}_2, 0})$ : essentially the two-link ‘plaquette,’ but with additional cutoff-enforcing projectors. The  $E_2$  components can then be eliminated just like before, by porting over  $\hat{\Xi}_{12}$  unchanged. Recalling how  $\hat{\Xi}_{12}$  transforms the operators  $\hat{U}_1\hat{U}_2^\dagger$ ,  $\hat{\mathcal{E}}_1$ , and  $\hat{\mathcal{E}}_2$ , we arrive at a sheared plaquette that is off-diagonal on register 1 alone:

$$\hat{U}_\square \xrightarrow{\Xi_{12}\Xi_{23}\Xi_{01}} = \hat{U}_1(1 - \delta_{\hat{\mathcal{E}}_2 - \hat{\mathcal{E}}_1, 0})(1 - \delta_{\hat{\mathcal{E}}_0 + \hat{\mathcal{E}}_1, -1}) \times (1 - \delta_{\hat{\mathcal{E}}_3 + \hat{\mathcal{E}}_2 - \hat{\mathcal{E}}_1, 0}). \quad (15)$$

Looking toward Trotterization, let us express the sheared plaquette as  $\hat{\lambda}_1^+\hat{\Pi}$ , where

$$\begin{aligned} \hat{\Pi} &\equiv [1 - \delta_{\hat{\mathcal{E}}_0 + \hat{\mathcal{E}}_1, -1}][1 - \delta_{\hat{\mathcal{E}}_1, -1}] \times \\ &\quad [1 - \delta_{\hat{\mathcal{E}}_2 - \hat{\mathcal{E}}_1, 0}][1 - \delta_{\hat{\mathcal{E}}_3 + \hat{\mathcal{E}}_2 - \hat{\mathcal{E}}_1, 0}]. \end{aligned}$$

$\hat{\Pi}$  is a projector on to the states in the electric hypercube not annihilated by  $\hat{U}_\square$ , after it has been sheared. Substituting for  $\hat{\lambda}^\pm$  and simplifying as in the toy example, we find that the Hamiltonian term that needs to be simulated in the sheared basis is given by

$$\hat{\Xi}_{12}\hat{\Xi}_{23}\hat{\Xi}_{01}(\hat{U}_\square + \hat{U}_\square^\dagger)\hat{\Xi}_{01}^\dagger\hat{\Xi}_{23}^\dagger\hat{\Xi}_{12}^\dagger = \hat{H}_e + \hat{H}_o, \quad (16)$$

$$\hat{H}_e = \hat{\Pi}_e X_1^{(\text{lsb})}, \quad (17)$$

$$\begin{aligned} \hat{\Pi}_e &\equiv [1 - \delta_{\hat{\mathcal{E}}_0 + 2\lfloor \hat{\mathcal{E}}_1/2 \rfloor, -1}] \times \\ &\quad [1 - \delta_{\hat{\mathcal{E}}_2 - 2\lfloor \hat{\mathcal{E}}_1/2 \rfloor, 0}][1 - \delta_{\hat{\mathcal{E}}_3 + \hat{\mathcal{E}}_2 - 2\lfloor \hat{\mathcal{E}}_1/2 \rfloor, 0}], \\ \hat{H}_o &= \hat{\lambda}_1^+\hat{\Pi}_o X_1^{(\text{lsb})} \hat{\lambda}_1^-, \end{aligned} \quad (18)$$

$$\begin{aligned} \hat{\Pi}_o &\equiv [1 - \delta_{\hat{\mathcal{E}}_0 + 2\lfloor \hat{\mathcal{E}}_1/2 \rfloor + 1, -1}][1 - \delta_{2\lfloor \hat{\mathcal{E}}_1/2 \rfloor + 1, -1}] \times \\ &\quad [1 - \delta_{\hat{\mathcal{E}}_2 - 2\lfloor \hat{\mathcal{E}}_1/2 \rfloor - 1, 0}][1 - \delta_{\hat{\mathcal{E}}_3 + \hat{\mathcal{E}}_2 - 2\lfloor \hat{\mathcal{E}}_1/2 \rfloor - 1, 0}]. \end{aligned}$$

Like in the two-link model,  $\hat{H}_e$  and  $\hat{H}_o$  are essentially controlled  $X$ -rotations on a single qubit, and they can be simulated separately in a Trotter-Suzuki expansion without violating gauge invariance. A quantum circuit for this (the counterpart to Fig. 5) is provided in the Supplemental Material.



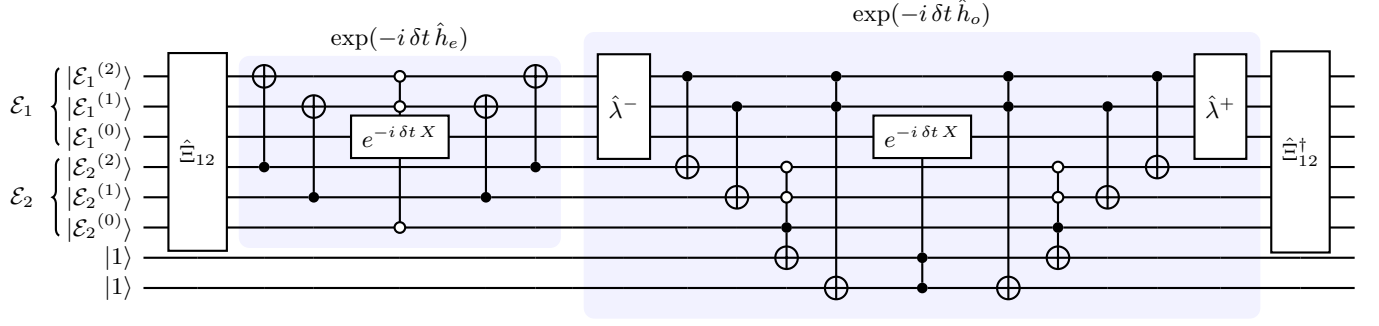


FIG. 5. Digital quantum circuit for gauge invariant, first-order Trotter-Suzuki approximation to  $\exp[-i \delta t (\hat{U}_1 \hat{U}_2^\dagger + \hat{U}_1^\dagger \hat{U}_2)]$  on a single toy plaquette (shown for  $\eta = 3$ ).

*Conclusion.*—The objective of this work was to furnish a new strategy for constructing digital quantum simulation algorithms for Abelian gauge theories that do not compromise gauge invariance. What makes gauge invariance nontrivial is the necessity of approximating time evolution with gates that generally are not gauge invariant, while at the same time enacting tightly correlated changes across many qubits. A key observation is that the particular transitions induced by a given gauge invariant interaction can be thought of as parallel edges of a spatial network in the space of involved charge quantum numbers. It follows that appropriately chosen cyclic shears can be used to align the edges parallel to the axis of a single quantum number, essentially converting the correlated changes across multiple qubit registers into controlled increments on a single register.

One obvious question remains: How practical is it to make the circuits gauge invariant? To this end, we will compare the sheared hopping propagator to its counterpart developed in Ref. [38]. As detailed in the Supplemental Material, an equitable comparison of the gate counting (in the approximation that  $\hat{U}$  is allowed to wrap around at the cutoff) leads to an upper bound of  $4\eta^2 + 20$  on the number of CNOTs called for within the shearing approach described in this work, as compared with the earlier CNOT upper bound of  $4\eta^2 - 4\eta + 18$ . The subleading cost increase (in  $\eta$ ) can, however, be avoided by an alternative choice of shears (also in the Supplemental Material), giving a final count of  $4\eta^2 - 4\eta + 20$  — just two more than the original algorithm. Given that the original circuit can induce unphysical transitions with probability as high as 0.8 if  $x \delta t$  grows to 1.8, and  $x \rightarrow \infty$  corresponds to the continuum limit of the Schwinger model, it would seem that two more CNOTs is a small price to pay to achieve the exact hopping propagator.

The operators studied in this work are important for compact U(1) gauge theories, but the shearing method's applicability could be broader. Key features that made the gauge invariant transitions tractable were the simultaneously diagonalizable constraints (guaranteeing basis states that can each be identified as allowed or unal-

lowed nodes), and the Cartesian structure of the truncated quantum numbers (which unitarily maps into itself under cyclic shears). Kogut-Susskind-like [80] formulations of nonabelian, SU(2) lattice gauge theory share neither of these: Gauss's law has noncommuting color components, and angular momentum quantum numbers  $\{j, m_L, m_R\}$  on links have a staggered pyramidal structure that does not naturally truncate to a box-like grid. The loop-string-hadron formulation of SU(2) lattice gauge theory [60], however, should be suitable for applications of shears because the same gauge invariant physics is encoded using strictly Abelian flux constraints and naturally-Cartesian quantum numbers.

Local gauge symmetries are most celebrated for their key role in defining the Standard Model of particle physics. The potential for simulating the Standard Model Hamiltonian efficiently, and with all known symmetries intact, will be an important clue as to whether or not our own universe could be a simulation [81] and further our insight into its intrinsic informational complexity. Could it be that optimal gauge invariant algorithms actually scale worse than optimal non-gauge invariant ones when it comes to extracting observables or to nonabelian gauge groups?

JRS thanks Zohreh Davoudi and Alexander Shaw for essential conversations that inspired this work and for valuable input on the manuscript. This research was supported by the US Department of Energy (DOE)'s Office of Science Early Career Award DE-SC0020271, and by the US DOE's Office of Science, Office of Advanced Scientific Computing Research, Accelerated Research in Quantum Computing program award DE-SC0020312.

\* [strykerj@umd.edu](mailto:strykerj@umd.edu)

- [1] M. Lüscher, Volume dependence of the energy spectrum in massive quantum field theories, *Commun.Math. Phys.* **105**, 153 (1986).
- [2] M. Lüscher, Two-particle states on a torus and their relation to the scattering matrix, *Nuclear Physics B* **354**,

- 531 (1991).
- [3] E. A. Martinez, C. A. Muschik, P. Schindler, D. Nigg, A. Erhard, M. Heyl, P. Hauke, M. Dalmonte, T. Monz, P. Zoller, and R. Blatt, Real-time dynamics of lattice gauge theories with a few-qubit quantum computer, *Nature* **534**, 516 (2016).
  - [4] N. Klco, E. F. Dumitrescu, A. J. McCaskey, T. D. Morris, R. C. Pooser, M. Sanz, E. Solano, P. Lougovski, and M. J. Savage, Quantum-classical computation of Schwinger model dynamics using quantum computers, *Phys. Rev. A* **98**, 032331 (2018).
  - [5] C. Kokail *et al.*, Self-verifying variational quantum simulation of lattice models, *Nature* **569**, 355 (2019), [arXiv:1810.03421 \[quant-ph\]](#).
  - [6] C. Schweizer, F. Grusdt, M. Berngruber, L. Barbiero, E. Demler, N. Goldman, I. Bloch, and M. Aidelsburger, Floquet approach to  $\mathbb{Z}_2$  lattice gauge theories with ultracold atoms in optical lattices, *Nat. Phys.* **15**, 1168 (2019).
  - [7] N. Klco, M. J. Savage, and J. R. Stryker, SU(2) non-Abelian gauge field theory in one dimension on digital quantum computers, *Phys. Rev. D* **101**, 074512 (2020).
  - [8] B. Yang, H. Sun, R. Ott, H.-Y. Wang, T. V. Zache, J. C. Halimeh, Z.-S. Yuan, P. Hauke, and J.-W. Pan, Observation of gauge invariance in a 71-site Bose–Hubbard quantum simulator, *Nature* **587**, 392 (2020).
  - [9] M. Kreshchuk, S. Jia, W. M. Kirby, G. Goldstein, J. P. Vary, and P. J. Love, Light-Front Field Theory on Current Quantum Computers, [arXiv:2009.07885](#) (2020).
  - [10] N. Klco and M. J. Savage, Minimally entangled state preparation of localized wave functions on quantum computers, *Phys. Rev. A* **102**, 012612 (2020), [arXiv:1904.10440](#).
  - [11] E. Gustafson, Y. Zhu, P. Dreher, N. M. Linke, and Y. Meurice, Real-time quantum calculations of phase shifts using wave packet time delays, [arXiv:2103.06848](#) (2021).
  - [12] C. W. Bauer, M. Freytsis, and B. Nachman, Simulating collider physics on quantum computers using effective field theories, [arXiv:2102.05044](#) (2021).
  - [13] Y. Atas, J. Zhang, R. Lewis, A. Jahanpour, J. F. Haase, and C. A. Muschik, SU(2) hadrons on a quantum computer, [arXiv:2102.08920](#) (2021).
  - [14] S. A. Rahman, R. Lewis, E. Mendicelli, and S. Powell, SU(2) lattice gauge theory on a quantum annealer, [arXiv:2103.08661](#) (2021).
  - [15] A. Ciavarella, N. Klco, and M. J. Savage, Trailhead for quantum simulation of SU(3) Yang-Mills lattice gauge theory in the local multiplet basis, *Phys. Rev. D* **103**, 094501 (2021), [arXiv:2101.10227](#).
  - [16] S. P. Jordan, K. S. M. Lee, and J. Preskill, Quantum Algorithms for Quantum Field Theories, *Science* **336**, 1130 (2012).
  - [17] S. P. Jordan, K. S. M. Lee, and J. Preskill, Quantum computation of scattering in scalar quantum field theories, *Quantum Information and Computation* **14**, 1014 (2014).
  - [18] A. Bhattacharyya, A. Shekar, and A. Sinha, Circuit complexity in interacting QFTs and RG flows, *J. High Energy Phys.* **2018** (10), 140.
  - [19] N. Klco and M. J. Savage, Digitization of scalar fields for quantum computing, *Phys. Rev. A* **99**, 052335 (2019), [arXiv:1808.10378 \[quant-ph\]](#).
  - [20] N. Klco and M. J. Savage, Systematically localizable operators for quantum simulations of quantum field theories, *Phys. Rev. A* **102**, 012619 (2020), [arXiv:1912.03577](#).
  - [21] J. Barata, N. Mueller, A. Tarasov, and R. Venugopalan, Single-particle digitization strategy for quantum computation of a  $\phi^4$  scalar field theory, *Phys. Rev. A* **103**, 042410 (2021), [arXiv:2012.00020](#).
  - [22] J. I. Cirac, P. Maraner, and J. K. Pachos, Cold Atom Simulation of Interacting Relativistic Quantum Field Theories, *Phys. Rev. Lett.* **105**, 190403 (2010).
  - [23] J. Casanova, L. Lamata, I. L. Egusquiza, R. Gerritsma, C. F. Roos, J. J. García-Ripoll, and E. Solano, Quantum Simulation of Quantum Field Theories in Trapped Ions, *Phys. Rev. Lett.* **107**, 260501 (2011).
  - [24] S. P. Jordan, K. S. M. Lee, and J. Preskill, Quantum Algorithms for Fermionic Quantum Field Theories, [arXiv:1404.7115](#) (2014).
  - [25] A. Hamed Moosavian and S. Jordan, Faster quantum algorithm to simulate fermionic quantum field theory, *Phys. Rev. A* **98**, 012332 (2018).
  - [26] NuQS Collaboration, H. Lamm, S. Lawrence, and Y. Yamauchi, Parton physics on a quantum computer, *Phys. Rev. Research* **2**, 013272 (2020).
  - [27] N. Mueller, A. Tarasov, and R. Venugopalan, Deeply inelastic scattering structure functions on a hybrid quantum computer, *Phys. Rev. D* **102**, 016007 (2020), [arXiv:1908.07051](#).
  - [28] S. Harmalkar, H. Lamm, and S. Lawrence, Quantum Simulation of Field Theories Without State Preparation, [arXiv:2001.11490](#) (2020).
  - [29] D. E. Kharzeev and Y. Kikuchi, Real-time chiral dynamics from a digital quantum simulation, *Phys. Rev. Research* **2**, 023342 (2020).
  - [30] B. Nachman, D. Provasoli, W. A. de Jong, and C. W. Bauer, Quantum Algorithm for High Energy Physics Simulations, *Phys. Rev. Lett.* **126**, 062001 (2021).
  - [31] Z. Davoudi, N. M. Linke, and G. Pagano, Toward simulating quantum field theories with controlled phonon dynamics: A hybrid analog-digital approach, [arXiv:2104.09346](#) (2021).
  - [32] M. C. Bañuls, R. Blatt, J. Catani, A. Celi, J. I. Cirac, M. Dalmonte, L. Fallani, K. Jansen, M. Lewenstein, S. Montangero, C. A. Muschik, B. Reznik, E. Rico, L. Tagliacozzo, K. Van Acoleyen, F. Verstraete, U.-J. Wiese, M. Wingate, J. Zakrzewski, and P. Zoller, Simulating lattice gauge theories within quantum technologies, *Eur. Phys. J. D* **74**, 165 (2020), [arXiv:1911.00003](#).
  - [33] T. Byrnes and Y. Yamamoto, Simulating lattice gauge theories on a quantum computer, *Phys. Rev. A* **73**, 022328 (2006).
  - [34] J. R. Stryker, Oracles for Gauss’s law on digital quantum computers, *Phys. Rev. A* **99**, 042301 (2019).
  - [35] NuQS Collaboration, H. Lamm, S. Lawrence, and Y. Yamauchi, General methods for digital quantum simulation of gauge theories, *Phys. Rev. D* **100**, 034518 (2019).
  - [36] NuQS Collaboration, A. Alexandru, P. F. Bedaque, S. Harmalkar, H. Lamm, S. Lawrence, and N. C. Warrington, Gluon field digitization for quantum computers, *Phys. Rev. D* **100**, 114501 (2019).
  - [37] E. Zohar and J. I. Cirac, Removing staggered fermionic matter in U(N) and SU(N) lattice gauge theories, *Phys. Rev. D* **99**, 114511 (2019).
  - [38] A. F. Shaw, P. Lougovski, J. R. Stryker, and N. Wiebe, Quantum Algorithms for Simulating the Lattice Schwinger Model, *Quantum* **4**, 306 (2020).
  - [39] B. Chakraborty, M. Honda, T. Izubuchi, Y. Kikuchi, and

- A. Tomiya, Digital Quantum Simulation of the Schwinger Model with Topological Term via Adiabatic State Preparation, [arXiv:2001.00485](#) (2020).
- [40] J. Liu and Y. Xin, Quantum simulation of quantum field theories as quantum chemistry, *J. High Energ. Phys.* **2020** (12), 11, [arXiv:2004.13234](#).
- [41] D. Paulson, L. Dellantonio, J. F. Haase, A. Celi, A. Kan, A. Jena, C. Kokail, R. van Bijnen, K. Jansen, P. Zoller, and C. A. Muschik, Towards simulating 2D effects in lattice gauge theories on a quantum computer, [arXiv:2008.09252](#) (2020).
- [42] NuQS Collaboration, Y. Ji, H. Lamm, and S. Zhu, Gluon field digitization via group space decimation for quantum computers, *Phys. Rev. D* **102**, 114513 (2020).
- [43] Z. Davoudi, I. Raychowdhury, and A. Shaw, Search for Efficient Formulations for Hamiltonian Simulation of non-Abelian Lattice Gauge Theories, [arXiv:2009.11802](#) (2020).
- [44] J. Bender and E. Zohar, Gauge redundancy-free formulation of compact QED with dynamical matter for quantum and classical computations, *Phys. Rev. D* **102**, 114517 (2020), [arXiv:2008.01349](#).
- [45] J. F. Haase, L. Dellantonio, A. Celi, D. Paulson, A. Kan, K. Jansen, and C. A. Muschik, A resource efficient approach for quantum and classical simulations of gauge theories in particle physics, *Quantum* **5**, 393 (2021).
- [46] A. Kan, L. Funcke, S. Kühn, L. Dellantonio, J. Zhang, J. F. Haase, C. A. Muschik, and K. Jansen, Investigating a 3+1D Topological  $\theta$ -Term in the Hamiltonian Formulation of Lattice Gauge Theories for Quantum and Classical Simulations, [arXiv:2105.06019](#) (2021).
- [47] E. Zohar and B. Reznik, Confinement and Lattice Quantum-Electrodynamical Electric Flux Tubes Simulated with Ultracold Atoms, *Phys. Rev. Lett.* **107**, 275301 (2011).
- [48] E. Zohar, J. I. Cirac, and B. Reznik, Quantum simulations of gauge theories with ultracold atoms: Local gauge invariance from angular-momentum conservation, *Phys. Rev. A* **88**, 023617 (2013).
- [49] E. Zohar and M. Burrello, Formulation of lattice gauge theories for quantum simulations, *Phys. Rev. D* **91**, 054506 (2015).
- [50] E. Zohar, A. Farace, B. Reznik, and J. I. Cirac, Digital Quantum Simulation of  $\mathbb{Z}_2$  Lattice Gauge Theories with Dynamical Fermionic Matter, *Phys. Rev. Lett.* **118**, 070501 (2017).
- [51] J. Bender, E. Zohar, A. Farace, and J. I. Cirac, Digital quantum simulation of lattice gauge theories in three spatial dimensions, *New J. Phys.* **20**, 093001 (2018).
- [52] Z. Davoudi, M. Hafezi, C. Monroe, G. Pagano, A. Seif, and A. Shaw, Towards analog quantum simulations of lattice gauge theories with trapped ions, *Phys. Rev. Research* **2**, 023015 (2020).
- [53] A. Mil, T. V. Zache, A. Hegde, A. Xia, R. P. Bhatt, M. K. Oberthaler, P. Hauke, J. Berges, and F. Jendrzejewski, A scalable realization of local U(1) gauge invariance in cold atomic mixtures, *Science* **367**, 1128 (2020).
- [54] D. Banerjee, M. Dalmonte, M. Müller, E. Rico, P. Stebler, U.-J. Wiese, and P. Zoller, Atomic Quantum Simulation of Dynamical Gauge Fields Coupled to Fermionic Matter: From String Breaking to Evolution after a Quench, *Phys. Rev. Lett.* **109**, 175302 (2012).
- [55] L. Tagliacozzo, A. Celi, A. Zamora, and M. Lewenstein, Optical Abelian lattice gauge theories, *Ann. Phys. (N. Y.)* **330**, 160 (2013).
- [56] A. Mezzacapo, E. Rico, C. Sabín, I. L. Egusquiza, L. Lamata, and E. Solano, Non-Abelian SU(2) Lattice Gauge Theories in Superconducting Circuits, *Phys. Rev. Lett.* **115**, 240502 (2015).
- [57] T. V. Zache, F. Hebenstreit, F. Jendrzejewski, M. K. Oberthaler, J. Berges, and P. Hauke, Quantum simulation of lattice gauge theories using Wilson fermions, *Quantum Sci. Technol.* **3**, 034010 (2018).
- [58] E. Zohar, J. I. Cirac, and B. Reznik, Cold-Atom Quantum Simulator for SU(2) Yang-Mills Lattice Gauge Theory, *Phys. Rev. Lett.* **110**, 125304 (2013).
- [59] M. Mathur and T. P. Sreeraj, Lattice Gauge Theories and Spin Models, *Phys. Rev. D* **94**, 085029 (2016), [arXiv:1604.00315](#).
- [60] I. Raychowdhury and J. R. Stryker, Loop, string, and hadron dynamics in SU(2) Hamiltonian lattice gauge theories, *Phys. Rev. D* **101**, 114502 (2020).
- [61] I. Raychowdhury and J. R. Stryker, Solving Gauss's law on digital quantum computers with loop-string-hadron digitization, *Phys. Rev. Research* **2**, 033039 (2020).
- [62] R. Dasgupta and I. Raychowdhury, Cold Atom Quantum Simulator for String and Hadron Dynamics in Non-Abelian Lattice Gauge Theory, [arXiv:2009.13969](#) (2020).
- [63] M. Kreshchuk, W. M. Kirby, G. Goldstein, H. Beauchemin, and P. J. Love, Quantum Simulation of Quantum Field Theory in the Light-Front Formulation, [arXiv:2002.04016](#) (2020).
- [64] A. Buser, H. Gharibyan, M. Hanada, M. Honda, and J. Liu, Quantum simulation of gauge theory via orbifold lattice, [arXiv:2011.06576](#) (2020).
- [65] R. P. Feynman, Simulating physics with computers, *Int. J. Theor. Phys.* **21**, 467 (1982).
- [66] S. Lloyd, Universal Quantum Simulators, *Science* **273**, 1073 (1996).
- [67] F. Arute, K. Arya, R. Babbush, D. Bacon, J. C. Bardin, R. Barends, R. Biswas, S. Boixo, F. G. S. L. Brandao, D. A. Buell, B. Burkett, Y. Chen, Z. Chen, B. Chiaro, R. Collins, W. Courtney, A. Dunsworth, E. Farhi, B. Foxen, A. Fowler, C. Gidney, M. Giustina, R. Graff, K. Guerin, S. Habegger, M. P. Harrigan, M. J. Hartmann, A. Ho, M. Hoffmann, T. Huang, T. S. Humble, S. V. Isakov, E. Jeffrey, Z. Jiang, D. Kafri, K. Kechedzhi, J. Kelly, P. V. Klimov, S. Knysh, A. Korotkov, F. Kostritsa, D. Landhuis, M. Lindmark, E. Lucero, D. Lyakh, S. Mandrà, J. R. McClean, M. McEwen, A. Megrant, X. Mi, K. Michielsen, M. Mohseni, J. Mutus, O. Naaman, M. Neeley, C. Neill, M. Y. Niu, E. Ostby, A. Petukhov, J. C. Platt, C. Quintana, E. G. Rieffel, P. Roushan, N. C. Rubin, D. Sank, K. J. Satzinger, V. Smelyanskiy, K. J. Sung, M. D. Trevithick, A. Vainsencher, B. Villalonga, T. White, Z. J. Yao, P. Yeh, A. Zalcman, H. Neven, and J. M. Martinis, Quantum supremacy using a programmable superconducting processor, *Nature* **574**, 505 (2019).
- [68] J. M. Chow, J. M. Gambetta, A. D. Córcoles, S. T. Merkel, J. A. Smolin, C. Rigetti, S. Poletto, G. A. Keefe, M. B. Rothwell, J. R. Rozen, M. B. Ketchen, and M. Steffen, Universal Quantum Gate Set Approaching Fault-Tolerant Thresholds with Superconducting Qubits, *Phys. Rev. Lett.* **109**, 060501 (2012).
- [69] S. Debnath, N. M. Linke, C. Figgatt, K. A. Landsman, K. Wright, and C. Monroe, Demonstration of a small programmable quantum computer with atomic qubits,

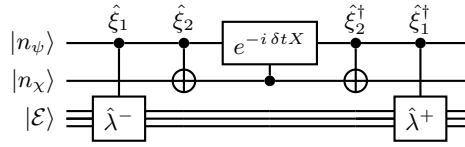


FIG. 6. Circuit to simulate a Schwinger model hopping term  $\hat{\psi}^\dagger \hat{\chi} \hat{U} + \text{H.c.}$  when the link operator is allowed to “wrap around” at the electric cutoffs.

- Nature** **536**, 63 (2016).
- [70] M. Reagor, C. B. Osborn, N. Tezak, A. Staley, G. Prawiroatmodjo, M. Scheer, N. Alidoust, E. A. Sete, N. Didier, M. P. da Silva, E. Acala, J. Angeles, A. Bestwick, M. Block, B. Bloom, A. Bradley, C. Bui, S. Caldwell, L. Capelluto, R. Chilcott, J. Cordova, G. Crossman, M. Curtis, S. Deshpande, T. E. Bouayadi, D. Girshovich, S. Hong, A. Hudson, P. Karalekas, K. Kuang, M. Lenihan, R. Manenti, T. Manning, J. Marshall, Y. Mohan, W. O’Brien, J. Otterbach, A. Papageorge, J.-P. Paquette, M. Pelstring, A. Polloreno, V. Rawat, C. A. Ryan, R. Renzas, N. Rubin, D. Russel, M. Rust, D. Scarabelli, M. Selvanayagam, R. Sinclair, R. Smith, M. Suska, T.-W. To, M. Vahidpour, N. Vodrahalli, T. Whyland, K. Yadav, W. Zeng, and C. T. Rigetti, Demonstration of universal parametric entangling gates on a multi-qubit lattice, *Science Advances* **4**, 10.1126/sciadv.aao3603 (2018).
- [71] U.-J. Wiese, Towards quantum simulating QCD, *Nucl. Phys. A Quark Matter 2014*, **931**, 246 (2014).
- [72] E. Zohar, A. Farace, B. Reznik, and J. I. Cirac, Digital lattice gauge theories, *Phys. Rev. A* **95**, 023604 (2017).
- [73] D. B. Kaplan and J. R. Stryker, Gauss’s law, duality, and the Hamiltonian formulation of U(1) lattice gauge theory, *Phys. Rev. D* **102**, 094515 (2020).
- [74] Y. Meurice, R. Sakai, and J. Unmuth-Yockey, Tensor field theory with applications to quantum computing, [arXiv:2010.06539](#) (2020).
- [75] M. C. Tran, Y. Su, D. Carney, and J. M. Taylor, Faster Digital Quantum Simulation by Symmetry Protection, *PRX Quantum* **2**, 010323 (2021).
- [76] J. C. Halimeh and P. Hauke, Staircase prethermalization and constrained dynamics in lattice gauge theories, [arXiv:2004.07248](#) (2020).
- [77] H. F. Trotter, On the product of semi-groups of operators, *Proc. Amer. Math. Soc.* **10**, 545 (1959).
- [78] M. Suzuki, Generalized Trotter’s formula and systematic approximants of exponential operators and inner derivations with applications to many-body problems, *Commun. Math. Phys.* **51**, 183 (1976).
- [79] A. M. Childs, Y. Su, M. C. Tran, N. Wiebe, and S. Zhu, Theory of Trotter Error with Commutator Scaling, *Phys. Rev. X* **11**, 011020 (2021).
- [80] J. Kogut and L. Susskind, Hamiltonian formulation of Wilson’s lattice gauge theories, *Phys. Rev. D* **11**, 395 (1975).
- [81] S. R. Beane, Z. Davoudi, and M. J. Savage, Constraints on the universe as a numerical simulation, *Eur. Phys. J. A* **50**, 148 (2014).

## SUPPLEMENTAL MATERIAL

### Alternate hopping circuit

The hopping circuit given in Fig. 2 implements the hopping propagator without approximation, but it apparently comes at an increased cost relative to the approximate circuit originally developed in Ref. [38]. To keep the comparison as straightforward as possible, we will allow the link operator to wrap around at the cutoff ( $\hat{U} |E_{\max}\rangle = |E_{\min}\rangle$ ) as was done in Ref. [38]. In a computational framework in which CNOTs were considered to be the “expensive” resource, the cost of a single hopping term propagator was found to be up to  $4\eta(\eta - 1) + 18$  CNOTs, where  $\eta$  is the number of qubits allocated to each electric link register. (For details, see §3.3 of Ref. [38]). Adapting that counting to the cutoff-wrapped hopping propagator in Fig. 6, we have:

- 2 explicit CNOTs
- 2 CNOTs used to implement the controlled  $e^{-ix\delta tX}$
- $2\eta^2$  CNOTS embedded in the controlled  $\hat{\lambda}^-$  [ $\eta(\eta - 1)$  for a quantum Fourier transform, plus another  $\eta(\eta - 1)$  for its inverse, plus an additional  $2\eta$  involved with adding the  $\chi$ -register control to  $\eta$  single-qubit rotations applied in Fourier space]
- $2\eta^2$  similarly for the controlled  $\hat{\lambda}^+$

This gives  $4\eta^2 + 4$  CNOTs in total. This is to be compared with  $4\eta^2 - 4\eta + 18$  CNOTs for the non-gauge-invariant algorithm. Based on the available information, the shear-based circuit in Fig. 6 increases the CNOT cost at subleading order in  $\eta$ , which can be attributed to the addition of a control to each basis incrementer  $\hat{\lambda}^\pm$ .



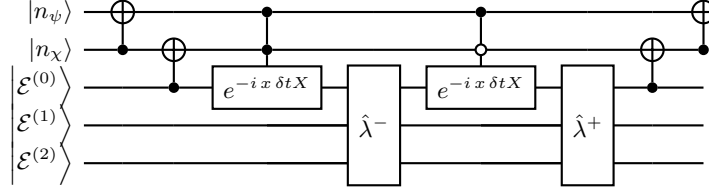


FIG. 7. Circuit to simulate a Schwinger model hopping term  $\hat{\psi}^\dagger \hat{\chi} \hat{U} + \text{H.c.}$ , shown here for a three-qubit electric register. The change of basis in this circuit involves two CNOTs, and while the interpretation of it as a shear of the quantum numbers is lost, the main guiding idea still applies: Each CNOT serves to help bring the edges parallel to a single axis.

If the shears in 2 and 3 increase the CNOT cost by calling for a control on the basis incrementers, we would like to know whether or not this is avoidable within the shearing approach. Note that the purpose of the controlled  $\hat{\lambda}^\pm$  gates was to induce a shear that removed the component of the graph edges along the  $E$  axis. This suggests that it may be advantageous to instead keep the edges'  $E$  components, taking the  $E$  axis as the one the edges are aligned to. Two alternative cyclic shears that will do this are

$$\begin{aligned}\hat{\xi}'_1 &= \delta_{\hat{n}_\chi,0} + X_\psi \delta_{\hat{n}_\chi,1} , \\ \hat{\xi}'_2 &= \sum_{j=0}^{2^\eta-1} \delta_{\hat{\mathcal{E}},j} (X_\chi)^j \\ &= \delta_{\hat{\mathcal{E}}(\bmod 2),0} + X_\chi \delta_{\hat{\mathcal{E}}(\bmod 2),1} ,\end{aligned}$$

where  $\xi'_1$  removes the edges' components along the  $n_\psi$  axis, and then  $\xi'_2$  removes the components along the  $n_\chi$  direction. We then have

$$\xi'_2 \xi'_1 (T_{\text{hop}} + T_{\text{hop}}^\dagger) \xi_1^\dagger \xi_2^\dagger = x \delta_{\hat{n}_\psi,1} \left[ \delta_{\hat{n}_\chi,0} \hat{\lambda}^+ X^{(\text{lsb})} \left( 1 - (\delta_{\hat{\mathcal{E}},-1} - \delta_{\hat{\mathcal{E}},-2}) \right) \hat{\lambda}^- + \delta_{\hat{n}_\chi,1} X^{(\text{lsb})} \right] .$$

In the cutoff-wrapped version, this term is simplified as

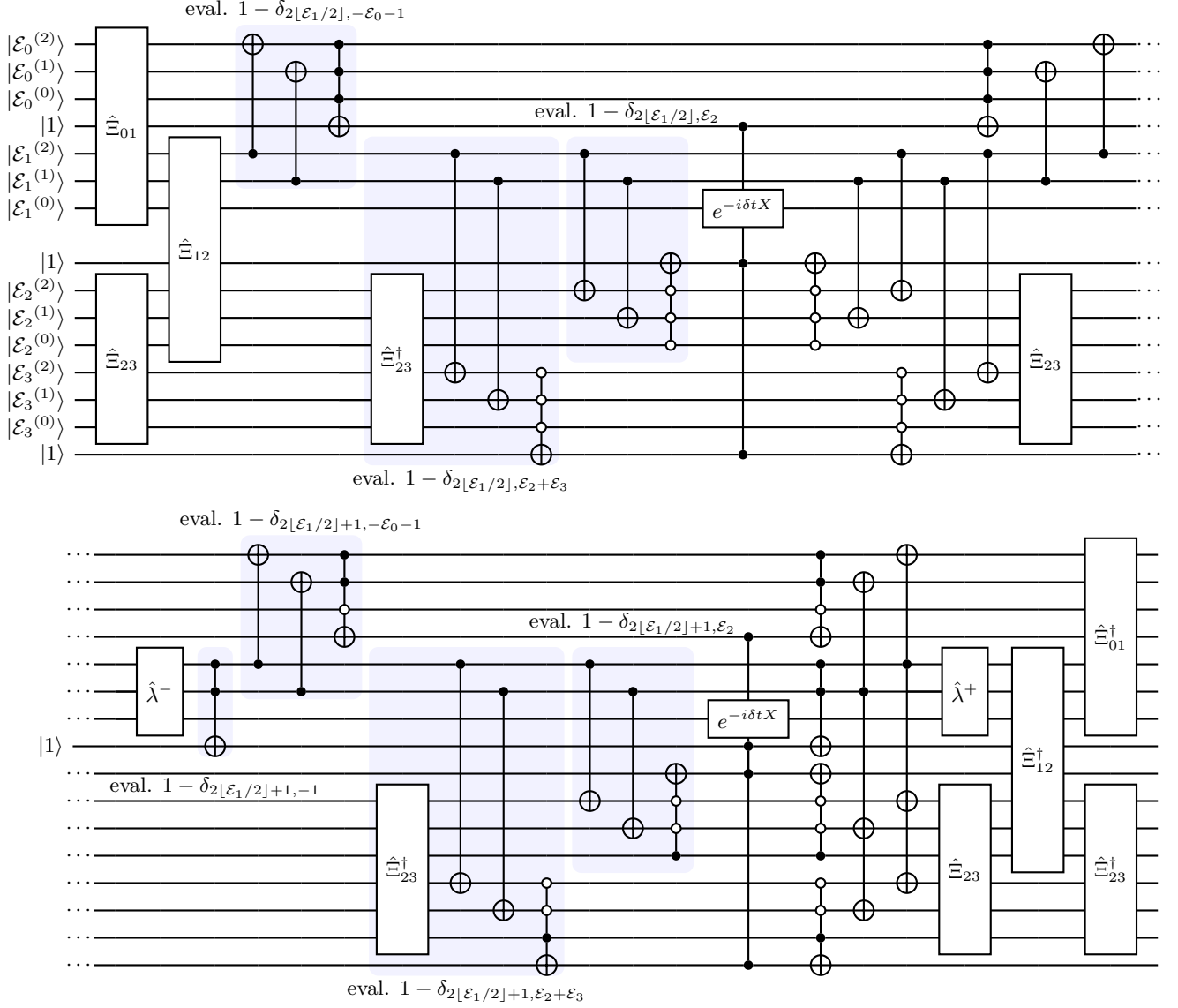
$$(T_{\text{hop}} + T_{\text{hop}}^\dagger) \xrightarrow{\text{wrapped } U} \xrightarrow{\xi'_2 \xi'_1} x \delta_{\hat{n}_\psi,1} \left[ \delta_{\hat{n}_\chi,0} \hat{\lambda}^+ X^{(\text{lsb})} \hat{\lambda}^- + \delta_{\hat{n}_\chi,1} X^{(\text{lsb})} \right] .$$

As desired, this term does not require controls on the incrementers. An exact circuit for it is shown in Fig. 7. The cost goes as follows:

- 4 explicit CNOTs
- 8 CNOTs for the doubly controlled  $e^{-i x \delta t X}$  gate
- 8 CNOTs for the doubly controlled  $e^{+i x \delta t X}$  gate
- $2\eta(\eta - 1)$  CNOTs for the  $\hat{\lambda}^-$  as done in Ref. [38]
- $2\eta(\eta - 1)$  CNOTs for the  $\hat{\lambda}^+$

This gives  $4\eta^2 - 4\eta + 20$  CNOTs in total, a constant increase of two relative to the old circuit. Additionally, the old circuit is accidentally exact for  $\eta < 3$ ; when we reach  $\eta = 3$ , 42 CNOTs are called for by the old circuit, which is much larger than the additional two needed to make the exact, gauge-conserving circuit.

Since we apparently have to pay more CNOTs for the new hopping term circuits, it is appropriate to ask what we are gaining in terms of the simulated physics. One way to answer this as follows: Suppose  $|\psi\rangle$  is some initial state in a definite charge sector,  $\mathcal{H}_{\text{phys}}$  is the space of states that can mix with  $|\psi\rangle$  under evolution by the exact hopping propagator, and  $\mathcal{H}_{\text{unphys}}$  is the orthogonal complement of  $\mathcal{H}_{\text{phys}}$ . Given that the approximate propagator circuit causes leakage into  $\mathcal{H}_{\text{unphys}}$  for  $\eta \geq 3$ , what is the worst-case probability (as a function of Trotter step time) of finding the evolved state in  $\mathcal{H}_{\text{unphys}}$ ? Numerically, we find that this probability can be as high as 0.8 if  $x \delta t$  grows as large as 1.8. In the continuum limit of asymptotically-free theories,  $x \rightarrow \infty$ , in which case  $\delta t$  has to shrink to keep the unphysical transitions suppressed.



**Four link circuit**

The circuit below, a generalization of Fig. 5 to the ordinary number of gauge links, represents the Trotterized propagator associated to a plaquette operator in a compact U(1) lattice gauge theory (discussed in the main text). In this case the plaquette operator is off-diagonal on four electric quantum numbers  $E_i$  ( $i = 0, 1, 2, 3$ ). The gauge invariant moves induced by  $U_\square + U_\square^\dagger$  can be thought of as edges running in the (1,1,-1,-1) direction of a four-dimensional grid. Shears in the 01- and 23-planes at the beginning of the circuit realign the edges to the (0,1,-1,0) direction. From that point forward, the circuit is essentially following the same steps as were taken for the two-link toy plaquette: propagating by the analogue of  $\hat{h}_e$  and then  $\hat{h}_o$ , with appropriate arithmetic and controls throughout serving to effect the electric cutoffs in a four-dimensional space.